



CHARACTERISTICS OF SELF-SIMILARITY OF SEISMICITY AND THE FAULT NETWORK OF THE SIKHOTE ALIN OROGENIC BELT AND THE ADJACENT AREAS

V. S. Zakharov^{1,2}, A. N. Didenko^{3,4}, G. Z. Gil'manova³, T. V. Merkulova³

¹ *M.V. Lomonosov Moscow State University, Faculty of Geology, Moscow, Russia*

² *Dubna State University, Dubna, Russia*

³ *Yu.A. Kosygin Institute of Tectonics and Geophysics, Far East Branch of RAS, Khabarovsk, Russia*

⁴ *Pacific National University, Khabarovsk, Russia*

Abstract: We performed a comprehensive analysis of the characteristics of self-similarity of seismicity and the fault network within the Sikhote Alin orogenic belt and the adjacent areas. It has been established that the main features of seismicity are controlled by the crustal earthquakes. Differentiation of the study area according to the density of earthquake epicenters and the fractal dimension of the epicentral field of earthquakes (D_e) shows that the most active crustal areas are linked to the Kharpi-Kur-Priamurye zone, the northern Bureya massif and the Mongol-Okhotsk folded system. The analysis of the earthquake recurrence plot slope values reveals that the highest b -values correlate with the areas of the highest seismic activity of the northern part of the Bureya massif and, to a less extent, of the Mongol-Okhotsk folded system. The increased fractal dimension values for the fault network (D_f) correlate with the folded systems (Sikhote Alin and Mongol-Okhotsk), while the decreased values conform to the depressions and troughs (Middle Amur, Uda and Torom). A comparison of the fractal analysis results for the fault network with the recent stress-strain data gives evidence of their general confinement to the contemporary areas of intense compression. The correspondence between the field of the parameter b -value for the upper crustal earthquakes and the fractal dimension value for the fault network (D_f) suggests a general consistency between the self-similar earthquake magnitude (energy) distribution and the fractal distribution of the fault sizes. The analysis results demonstrate that the self-similarity parameters provide an important quantitative characteristic in seismotectonics and can be used for the neotectonic and geodynamic analyses.

Key words: seismicity; earthquake epicentres; earthquake recurrence plot; fault network; self-similarity; fractal dimension; neotectonics; geodynamics

RESEARCH ARTICLE

Received: December 12, 2018

Revised: April 30, 2019

Accepted: May 23, 2019

For citation: Zakharov V.S., Didenko A.N., Gil'manova G.Z., Merkulova T.V., 2019. Characteristics of self-similarity of seismicity and the fault network of the Sikhote Alin orogenic belt and the adjacent areas. *Geodynamics & Tectonophysics* 10 (2), 541–559. doi:10.5800/GT-2019-10-2-0425.

ХАРАКТЕРИСТИКИ САМОПОДОБИЯ СЕЙСМИЧНОСТИ И РАЗЛОМНОЙ СЕТИ СИХОТЭ-АЛИНЬСКОГО ОРОГЕННОГО ПОЯСА И ПРИЛЕГАЮЩИХ ТЕРРИТОРИЙ

В. С. Захаров^{1,2}, А. Н. Диденко^{3,4}, Г. З. Гильманова³, Т. В. Меркулова³

¹ Московский государственный университет им. М.В. Ломоносова, геологический факультет, Москва, Россия

² Государственный университет «Дубна», Дубна, Россия

³ Институт тектоники и геофизики им. Ю.А. Косыгина ДВО РАН, Хабаровск, Россия

⁴ Тихоокеанский государственный университет, Хабаровск, Россия

Аннотация: Проведен комплексный анализ характеристик самоподобия сейсмичности и сети разломов в пределах Сихотэ-Алинского орогенного пояса и прилегающих территорий. Установлено, что основные особенности сейсмичности определяются коровыми землетрясениями. Дифференциация исследуемой территории по плотности эпицентров и величине фрактальной размерности поля эпицентров (D_e) показывает, что наиболее активные участки земной коры связаны с Харпийско-Курско-Приамурской зоной, с северной частью Буреинского массива и Монголо-Охотской складчатой системой. Анализ значений наклона графика повторяемости землетрясений (b) показывает, что наибольшие его величины соответствуют районам наибольшей сейсмической активности: северной части Буреинского массива и, в меньшей степени, – Монголо-Охотской системе. Повышенные значения фрактальной размерности разломной сети (D_f) соответствуют складчатым системам (Сихотэ-Алинской и Монголо-Охотской), а пониженные – впадинам и прогибам (Среднеамурская, Удский и Торомский). Сопоставление результатов фрактального анализа сети разломов с данными по современному напряженно-деформированному состоянию показывает их общую приуроченность к областям интенсивного современного сжатия. Соответствие поля параметра b для верхнекоровых землетрясений и поля размерности сети разломов D_f указывает на общую согласованность самоподобного распределения магнитуды (энергии) землетрясений и фрактального распределения размеров разрывных нарушений. Полученные результаты показывают, что параметры самоподобия являются важной количественной характеристикой в сейсмотектонике и могут использоваться при неотектоническом и геодинамическом анализе.

Ключевые слова: сейсмичность; эпицентры землетрясений; график повторяемости; сеть разломов; самоподобие; фрактальная размерность; неотектоника; геодинамика

1. INTRODUCTION

The Sikhote Alin orogenic belt is located in the eastern part of the Amurian plate, its structures are stretching from the Sea of Okhotsk coast in the north to the Sea of Japan coast in the south (Fig. 1, a). From the east, the belt is separated from Sakhalin Island by the rift structure of the Tatar Strait. In the west, it is flanked by the Bureya and Khanka ancient massifs covered with Early Paleozoic continental crust, and bordered by the Jurassic Mongol-Okhotsk fold-nappe belt in the northwest [Didenko et al., 2010]. The Mesozoic-Cenozoic geodynamics of the region, its tectonic structure and recent movements were and are currently controlled by the interaction between the continental Eurasian and Amurian, the subcontinental Okhotsk and oceanic Pacific tectonic plates [Khanchuk, 2006]. In this region, seismicity is caused by the two main processes. In the eastern part, it is the Pacific Plate subduction beneath the Okhotsk and Amurian plates. In the western part,

seismicity is due to the interaction between different blocks of the Amurian plate along NNE-striking Kharpi-Kur-Primurye fault system (the northern segment of the Tan-Lu Fault System) and the Central Sikhote Alin Fault [Khanchuk, 2006; Didenko et al., 2017; Levin et al., 2008; Stepashko et al., 2018].

As compared to the westerly lying Kuril-Kamchatka and Japan subduction zones, the study area is considerably less seismically active, yet characterized by quite appreciable seismic activity. Relatively few works are focused on the detailed analysis of contemporary seismicity of the Sikhote Alin region and the controlling active tectonic structures [e.g., Nikolaev, 1992; Khanchuk, 2006; Levin et al., 2008; Ulomov, 2009; Gorelov et al., 2016; Safonov, 2018]. But the subject seems to be quite topical, firstly, because paleoseismological data revealed up to M 7.3 earthquakes that occurred here in the recent geological past (Holocene) [Ovsyuchenko et al., 2018], and, secondly, a series of M 6.1–7.5 earthquakes including the catastrophic ones were recorded

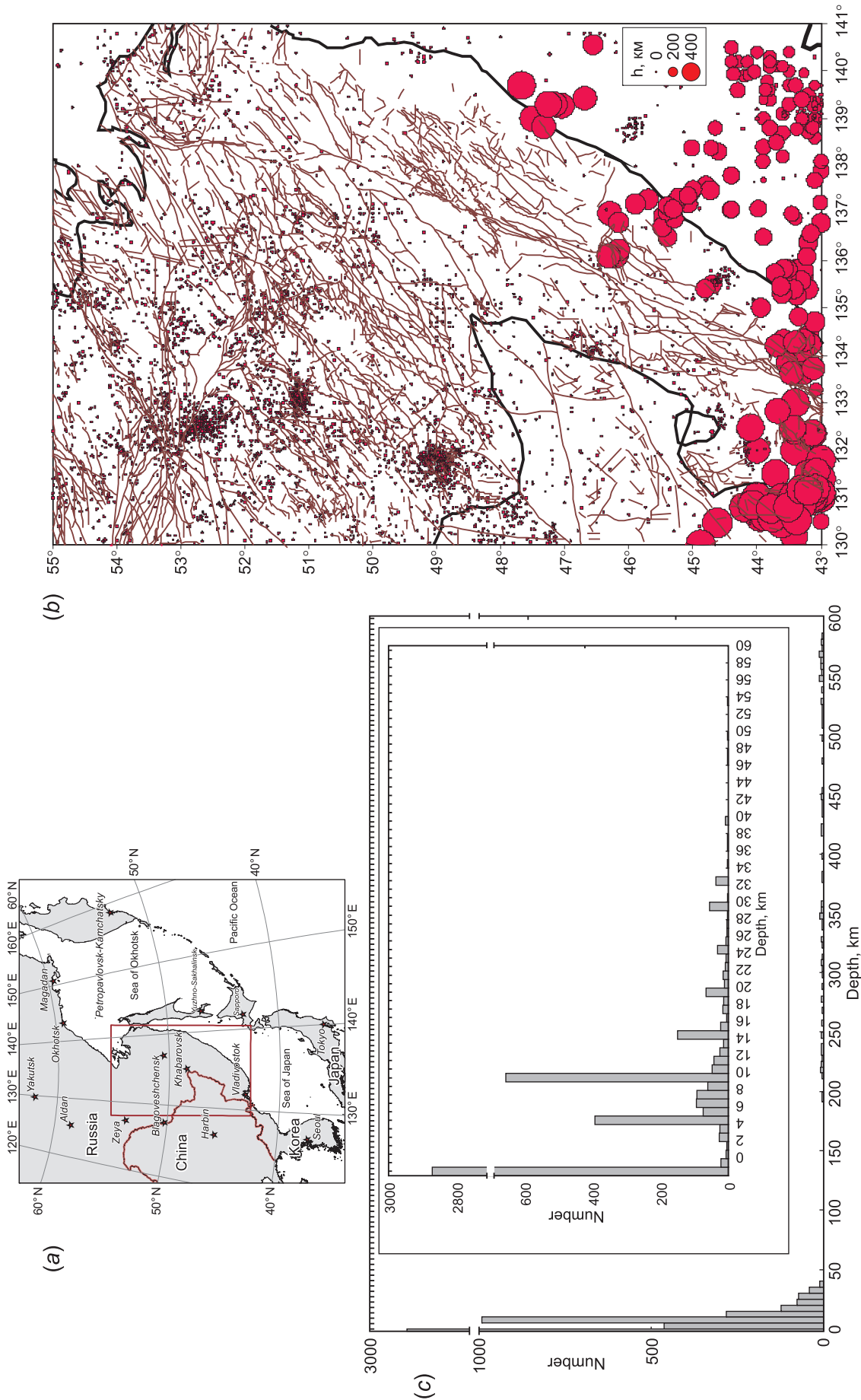


Fig. 1. Seismicity and faults in the study area. (a) – study area on the map of East Eurasia (frame); (b) – earthquake epicenters (the circle sizes are proportional to the focal depth) and faults (thin lines) (after [Zabrodin et al., 2015]); (c) – depth distribution of earthquakes. The insert shows a more detailed earthquake distribution in a depth range of 0–60 km; the vertical scale is broken.

Рис. 1. Сейсмичность и разломы района исследования. (a) – изученная территория на карте востока Евразии (рамка); (b) – положение эпицентров землетрясений (размер кругов пропорционален глубине очага) и разломов (тонкие линии), по [Zabrodin et al., 2015]; (c) – распределение землетрясений по глубине, на врезке более детально показано распределение в диапазоне глубин 0–60 км, вертикальная шкала имеет разрыв.

in the southern segment of the Tan-Lu Fault zone in the territory of China in the 1960s and 1970s.

The hierarchical properties of seismicity and various-scale faults in different regions were investigated by a great number of the Russian and foreign researchers [e.g., *Sadovsky, Pisarenko, 1991; Robertson et al., 1995; Turcotte, 1997; Goryainov, Ivanyuk, 2001; Sherman et al., 2001; Sadovsky, 2004; Kossobokov, Nekrasova, 2004; Nekrasova, Kossobokov, 2005; Stakhovsky, 2004, 2017; Sherman, 2005, 2012; 2014; Ben-Zion, 2008; Torabi, Berg, 2011; Nekrasova et al., 2015; and many others*]. These properties are expressed by the power laws that relate different characteristics of the fault structures and the associated seismicity. Applying fractal geometry approaches to fault tectonics considerably increases the capabilities of applied numerical methods. For example, the possibilities of such an approach were demonstrated by performing the analysis of the self-similarity characteristics for the active fault network of Eurasia in their close relationship with the seismicity characteristics [Zakharov, 2011].

The goal of our study is to perform a comprehensive analysis of the characteristics of self-similarity of seismicity and the fault network within the Sikhote Alin orogenic belt and the adjacent areas, and compare these characteristics between each other and with tectonic and geodynamic features of the region. In this paper, we proceed to present the results of our studies focused on seismotectonics of the region and based on approaches of the theory of dynamic systems and fractals that were initiated by *Didenko et al. [2017]*.

2. INPUT DATA

The study area is bounded by 43–55° N and 129–141° E (Fig. 1). The earthquake catalog created by the Laboratory of Seismology and Seismotectonics at the Institute of Tectonics and Geophysics, Far East Branch, Russian Academy of Sciences (ITiG FEB RAS) was used as the main source of data on the seismicity of the region. It is based on the data on the Primorye and Priamurye earthquakes derived from [Kondorskaya, Shebalin, 1977] and collections [Earthquakes in Russia, 2006–2013; Earthquakes of North Eurasia, 1992–2013; Earthquakes in the USSR, 1962–1991]. A total of 5177 earthquakes occurred from 1500 to 2013 have been analyzed (Fig. 1, b). The catalog compiled by ITiG FEB RAS provides the information on the earthquake origin time, hypocenter coordinates and M_{LH} magnitude (magnitude on LH waves). The magnitudes of part of earthquakes were determined by recalculating their energy class into M_{LH} [Rautian et al., 2007]. This catalog lists individual rare seismic events occurred before 1960, which main parameters were determined from macroseismic data. It should be noted

that the number of recorded events has increased with the development of the regional network of seismic stations. The most representative datasets were obtained in 1975–1992, when the network of regional seismic stations allowed for reliable recording of up to 7–8 energy class earthquakes ($M_{LH}=2.4-2.8$). It is most likely that just because of this reason the events with $M \geq 2.4$ were listed in the initial catalogs in the following years. We also used the seismic events with $M_{LH} \geq 2.4$ in our calculations.

Based on the analysis of earthquake hypocenter depths in the region, performed by *Levin et al. [2008]*, *Khanchuk [2006]* and others, the earthquakes can be subdivided at least into two groups – crustal and mantle. The latter are grouped in the southern and south-eastern parts of the region and are related to the oceanic Pacific Plate subduction beneath the Eurasian eastern margin. In this paper, we do not consider them as a subject of the study. In the region, the seismicity is mainly controlled by the crustal earthquakes caused by the recent crustal fault-block tectonic activity. Figure 1c shows the depth distribution of earthquakes based on the earthquake catalog data. It is seen that the absolute majority of the earthquake foci (a total of 4937, i. e., 95 %) are of no greater than 36 km depth. Note that in the catalog, about half of the events (a total of 2890) show the (-1) depth and thus refer to the surface earthquakes, for which it does not appear possible to determine a precise occurrence depth. Besides, the narrow maxima are confined to 5, 10, and 15 km focal depth range, which are also due to the lack of possibility to precisely determine the depths for part of the earthquakes.

In the study area, the crustal thickness varies within 14–38 km according to the model CRUST 2.0 [CRUST 2.0]. Therefore, when further analyzing seismicity, the earthquakes with the focal depths not exceeding 36 km were referred to the crustal earthquakes. Note that the upper crustal earthquakes with the focal depths of no more than 12 km are prevalent among the crustal earthquakes (see Fig. 1, c). The number of such events is as large as 4433, which amounts to 85 % of the total number of all the analyzed earthquakes, and to 90 % of the crustal ones. Such earthquake distribution is well consistent with the upper crustal thickness reaching 10–12 km in this area according to the model CRUST 2.0. This feature is important for a comparison of the characteristics of self-similarity of seismicity with similar characteristics for the fault network. We will mainly compare the characteristics of fault tectonics displayed at the surface (fault network) with the characteristics of the crustal and upper crustal seismicity.

To perform the analysis and to compare the characteristics of seismicity, we used the digital map of faults (vector form, see Fig. 1, b) and their descriptions pre-

pared by *Zabrodin et al.* [2015] as the initial fault data for the region including the data on active faults, which are available at (http://itig.as.khb.ru/ppl/gis/2015-mono-Fault_Tect_FE-Zabr_Ry_Gil.pdf).

3. ANALYSIS TECHNIQUE

The spatial structure of the epicentral field of earthquakes is rather complicated and nonuniform, and these properties are displayed in a broad scale range, that is, self-similarity, or fractality, takes place [Mandelbrot, 1983]. Without consideration to the size of an earthquake focus, a set of the earthquake foci has the character of the Cantor (point) sets. Fractal dimension D is a quantitative measure of self-similarity and a degree of complexity of a set of objects [Sadovsky, Pisarenko, 1991; Turcotte, 1997], which shows how densely and uniformly the space is filled with the elements of a set given, and is calculated from the relation:

$$\lg N = -D \lg \delta + c_1, \tag{1}$$

where δ is the scale of consideration, N is the number of elements, c_1 is the constant.

To analyze the fractal dimension of the epicentral field of earthquakes D_e , we used the box counting (BC) method. Following that method, the analyzed set of points is covered with boxes of size δ , and the dependence of a kind (1) is constructed that relates the number of boxes N , where even one point of a set falls in, with a scale δ . A similar method is described in the patent [Klyuchevskiy et al., 2017]. The square sites were used which minimum size was determined based on the data detail and attained 0.125° by latitude, whereas the maximum size stemmed from the need to stack a number of sites within the overall domain size and to provide no less than one order of scale variation to perform the analysis. In our calculations, we took into account the boxes within which no less than one earthquake fell. The regression equation was solved using the least squares method (LSM). Figure 2, *a*, illustrates an example showing the calculation of the fractal dimension of the epicentral field of earthquakes D_e in the region.

In terms of energy characteristics, self-similarity of the seismic regime is attested by the Gutenberg-Richter (GR) law for the magnitude distribution of a number of earthquakes which is of fundamental importance in seismology [Kasahara, 1981]:

$$\lg N = -b \lg M + a, \tag{2}$$

where a and b are empirical constants, N is the number of earthquakes with the magnitude exceeding M for a certain time period in a given region. This relation

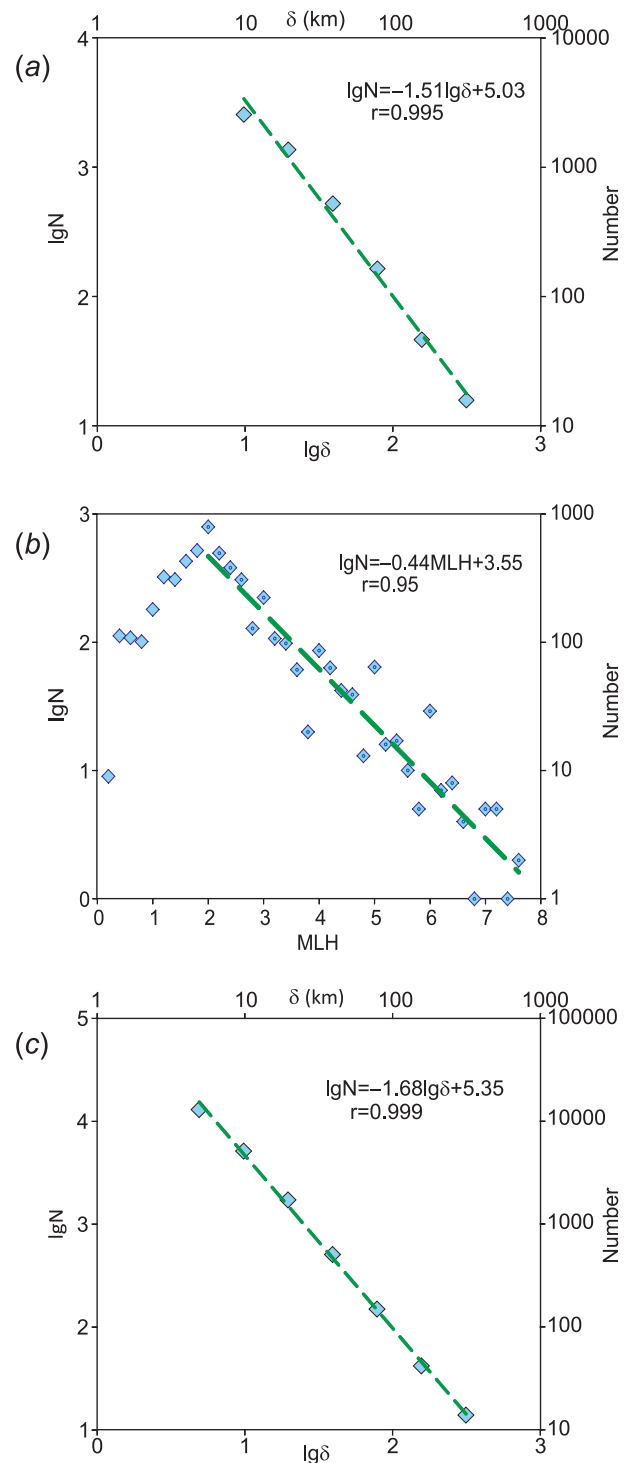


Fig. 2. Calculation of self-similarity parameters. (a) – calculation of the fractal dimension of the epicentral field $D_e=1.51\pm 0.08$; (b) – M_{LH} magnitude distribution of earthquakes and determination of parameter $b=0.44\pm 0.03$; (c) – fractal dimension of the fault network, $D_f=1.68\pm 0.03$.

Рис. 2. Определение параметров самоподобия, используемых в работе. (a) – вычисление фрактальной размерности поля эпицентров $D_e=1.51\pm 0.08$; (b) – распределение землетрясений по магнитудам M_{LH} и определение наклона графика повторяемости $b=0.44\pm 0.03$; (c) – определение фрактальной размерности сети разломов $D_f=1.68\pm 0.03$.

holds for the decay area of the distribution plot $\lg N(M)$, the earthquake recurrence plot, showing the relation between the number of weak and strong seismic events occurred in the region. The parameter b -value can be calculated using different methods, such as the maximum likelihood estimation (MLE) (e. g. [Nava et al., 2017]) or the least squares method (LSM). As mentioned above, we used the LSM in our study, a discrete step size for the earthquake magnitude attained 0.2 unit. Figure 2, *a*, illustrates an example of the non-cumulative recurrence plot construction and the parameter b -value estimation for the region.

The investigations of the distribution laws for a number of faults N (and other fault structures) according to their length L in different regions and various geodynamic environments by different authors [e.g. Sadovsky, Pisarenko, 1991; Sherman, 2005, 2012, 2014; and others] have clarified that these laws are described by a power-law relation of the following kind:

$$N \sim L^{-m},$$

where m is the power exponent, i. e. they are of the fractal character. To calculate the fractal dimension of the fault network D_f , we used the above described box counting method and the following relation was applied:

$$\lg N = -D_f \lg \delta + c_2, \quad (3)$$

where δ is the scale of consideration, N is the box number, c_2 is the constant. During the analysis, the square sites were used whose sizes and the variation range were taken the same as for the calculation of the fractal dimension of the field of earthquake epicenters D_e . In order to make the comparison of the results correct. The regression equation was solved using the least squares method. Figure 2, *a*, depicts an example of the fractal dimension of the fault network D_f in the region.

4. CHARACTERISTICS OF SELF-SIMILARITY OF SEISMICITY

4.1. ANALYSIS OF EPICENTER DENSITY

Before we start analyzing the characteristics of self-similarity of seismicity, the conventionally assumed indicator of seismic activity such as the surface density of earthquake epicenters has been analyzed. This value attains $0.33 \cdot 10^{-2} \text{ km}^{-2}$, on average, but it is however extremely nonuniformly distributed in the study area. To reveal the spatial pattern of seismicity, we calculated the surface density over a moving window of 2° size by latitude (approximately $160 \times 160 \text{ km}$ at a given latitude) with a step of 0.5° (40 km) using the author's FrAnGeo program [Zakharov, 2011, 2012]. The results

are presented in Fig. 3. There are practically no differences in the densities of both crustal and upper crustal earthquake epicenters, which results from complete prevalence of the number of the upper crustal and crustal seismic events over the mantle ones.

The statistics of the surface density distribution of earthquake epicenters is shown in Fig. 3, *b*. The distribution pattern is considerably different from the 'normal' one: the minimum value is 0, the maximum value is $2.81 \cdot 10^{-2} \text{ km}^{-2}$, and the median is $0.36 \cdot 10^{-2} \text{ km}^{-2}$. Furthermore, the distribution is bimodal. In addition to the main maximum observed at low density values consistent with the seismically inactive or weakly active zones, the explicit maximum is displayed in a range of $1.7\text{--}1.9 \cdot 10^{-2} \text{ km}^{-2}$, although with a lower amplitude that correlates with the areas of increased seismic activity.

The obtained results are well consistent with the earlier results presented in Didenko et al. [2017], and Stepashko et al. [2018]. They provide evidence that in terms of seismicity manifestation, the study area is rather nonuniform. Variations in the surface density of the earthquake foci (see Fig. 3, *a*) indicate that the most seismically active crustal areas showing the highest density values in the earthquake epicenter distribution are linked to NE-trending Kharpi-Kur-Priamurye zone, that is the northern segment of the transregional Tan-Lu Fault System [Nikolaev, 1992; Khanchuk, 2006]. Based on the highest occurrence frequency of the seismic events, four areas have been distinguished here (from south to north): (1) between the Kukan Mountain Range and the southwestern branch of the Bureya Mountain Range; (2) at the southern foothills of the Turan Range; (3) at the northeastern branch of the Bureya Range; and (4) the area between the Ezop, Yam Alin and Seledzha Ranges. The latter area exhibits the highest density value in the earthquake epicenter distribution in the region.

In contrast to the Kharpi-Kur-Priamurye zone, we do not observe crustal zones of similar seismicity within the Sikhote Alin orogen. Here, the exceeding background seismicity can be observed in the following areas (from north to south, see Fig. 3): (1) the lower reaches of the Amur River near Nikolaevsk-on-Amur; (2) the water area of the Sea of Japan, specifically Svetlaya and Maksimovka Bays; and (3) southern Primorye. The most seismically active areas near Vladivostok and Olga Bay are most likely related to the subduction zones.

4.2. FRACTAL DIMENSION ANALYSIS OF THE FIELD OF EARTHQUAKE EPICENTERS

Using the FrAnGeo program [Zakharov, 2011, 2012] and the box counting method, the fractal dimension of the distribution of earthquake epicenters D_e was calculated from relation (1) for all the seismic events

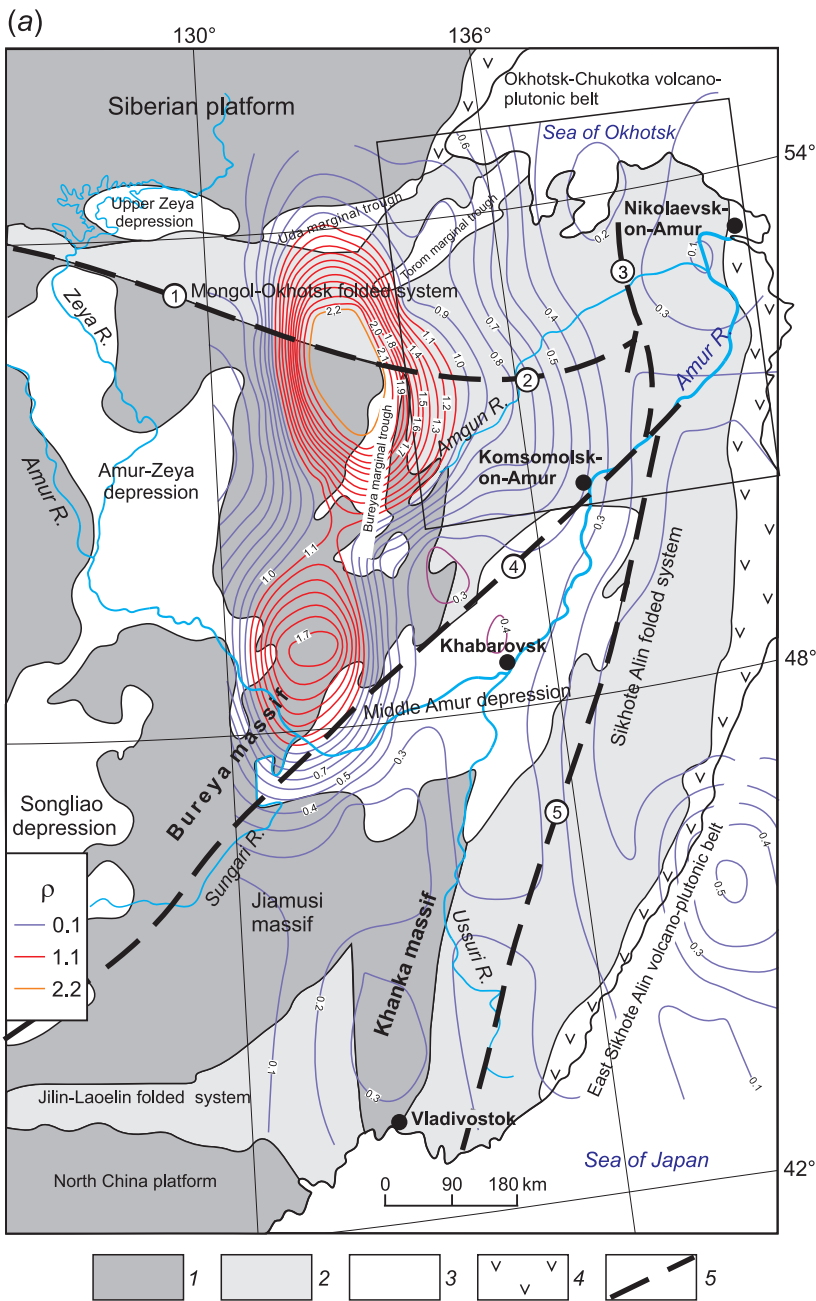
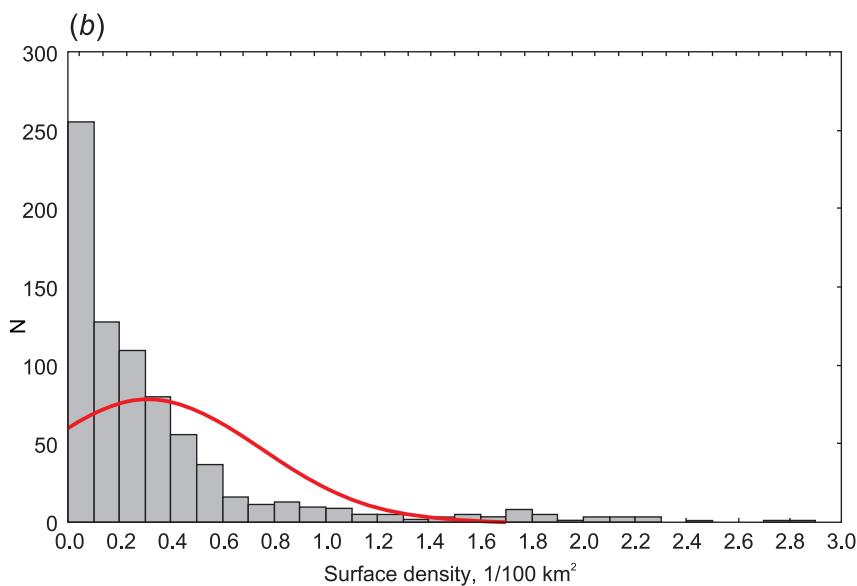


Fig. 3. Density of earthquake epicenters.

(a) – spatial variations in the density of the crustal earthquake epicenters ρ (per 100 km² area) compared to the structural scheme of the region (after [Zabrodin, 2017]): 1 – Precambrian platforms; 2 – Phanerozoic folded systems; 3 – Cenozoic depressions; 4 – volcano-plutonic systems; 5 – faults (figures in the circles: 1 – South Tukuringra, 2 – Paukan, 3 – Limurchan, 4 – Yitong-Yilan, 5 – Central Sikhote Alin); (b) – distribution of the surface density of earthquake epicenters, the red line shows the normal distribution with the same average value and dispersion.

Рис. 3. Плотность эпицентров землетрясений.

(a) – пространственные вариации плотности эпицентров ρ (на 100 км²) коровых землетрясений в сопоставлении со структурной схемой региона, по [Zabrodin, 2017]: 1 – докембрийские платформы; 2 – складчатые системы фанерозоя; 3 – кайнозойские впадины; 4 – вулканоплутонические системы; 5 – разломы (номера в кругах: 1 – Южно-Тукурингрский, 2 – Пауканский, 3 – Лимурчанский, 4 – Итунь-Илань, 5 – Центральный Сихотэ-Алинский); (b) – распределение значений поверхностной плотности эпицентров землетрясений, красной линией показано нормальное распределение с теми же средним значением и дисперсией.



recorded in the study area irrespective of their magnitudes. The range of box sizes used for calculating D_e varied from 4 to 0.125° by latitude (approximately 315–10 km). The fractal dimension of the entire field of earthquake epicenters was estimated to be $D_e=1.51\pm 0.08$ (see Fig. 2, *a*; the correlation coefficient $r=0.99$). For the crustal earthquakes, $D_e=1.49\pm 0.07$ ($r=0.99$), whereas for the upper crustal earthquakes, $D_e=1.46\pm 0.07$ ($r=0.99$), respectively. This exhibits a certain refinement of our earlier results [Didenko et al., 2017], according to which the fractal dimension of the epicentral field of all the analyzed earthquakes and the crustal ones attained $D_e=1.6\pm 0.1$, while the fractal dimension of the upper crustal seismicity was not estimated.

Summing up, the above mentioned estimates coincide within the calculation error, and the general structure of the geometric self-similarity of the field of earthquake epicenters is mainly controlled by the crustal earthquakes. In the study area, high values of D_e indicate that the structure of the epicentral field of earthquakes has a rather complicated distributed pattern in the range of two orders of spatial scale.

To reveal the spatial features of variations in the fractal dimension of the epicentral field of earthquakes, we performed more detailed moving window calculations using the author's FrAnGeo program as compared to the earlier calculations presented in Didenko et al. [2017]. The window size was 2° by latitude (approximately 160×160 km), a step was 0.5° (40 km), and the range of box sizes was 2–0.125° by latitude (160–10 km). The calculated field of D_e for the upper crustal earthquakes is shown in Fig. 4. Differentiation of the study area based on the fractal dimension value shows that zones of the highest values of D_e , generally correlate with seismically active crustal areas determined from the surface density of the earthquake foci.

4.3. MAGNITUDE DISTRIBUTION OF EARTHQUAKES AND THE PARAMETER b -VALUE OF THE RECURRENCE PLOT

The recurrence plot was constructed for all the earthquakes recorded in the region (see Fig. 2, *b*). The parameter b -value was calculated from relation (2) in a magnitude range of 2.2–7.6, and $b=0.44\pm 0.03$ ($r=0.95$). The magnitude distribution of the crustal earthquakes is appreciably different from the overall distribution: $b=0.60\pm 0.03$ ($r=0.97$), whereas for the upper crustal earthquakes $b=0.69\pm 0.04$ ($r=0.97$), respectively. This is because in the region, the maximum magnitudes of all the crustal earthquakes do not exceed 7, while for the upper crustal earthquakes this value is 6.4. The lack of stronger earthquakes is shown by a greater slope of the recurrence plot.

In addition to the general b -value estimation for the region, more detailed moving window calculations of

the b -value field were performed as compared to the calculations reported in our previous work [Didenko et al., 2017]. The moving window size was 2° by latitude (160×160 km), a step was 0.5° (40 km) and the range of box sizes used for the calculations varied from 2 to 0.125° (160–10 km).

The field of the recurrence plot slope values for the crustal earthquakes (Fig. 5, *a*) demonstrates that the highest absolute value (≥ 0.7) correlates with the areas of disjunctive faults developed in the northern Bureya massif and NE-trending Kharpi-Kur-Priamurye zone, that is the northern segment of the transregional Tan-Lu Fault System [Nikolaev, 1992; Khanchuk, 2006]. Another maximum of the parameter b -value is exhibited for the central Sikhote Alin zone. The minimum recurrence plot slope values fall in the southern and northern Sikhote Alin zones. The b -value field for the crustal earthquakes mainly differs from that for all the studied earthquakes by the presence of the b -value maximum in the Sea of Japan (at the shelf boundary). Apparently, this is because relatively strong earthquakes are rather of mantle than crustal origin in this area, which is displayed in higher b -values estimated for the crustal earthquakes.

The b -value distribution for the upper crustal earthquakes (Fig. 5, *b*) is quite close to the 'normal' one (except for the lowest b -value area, the minimum value is 0.20, the maximum value is 1, the average value amounts to 0.49 ± 0.02 , the standard deviation is 0.15, and the median of the distribution is 0.48). Let us point out that at $b=0.65$, a step appears on the recurrence plot, which value may be used as a threshold value to distinguish the highest b -value area.

The results of comparison of the parameter b -value field and the fractal dimension of the earthquake epicenters D_e are shown in Fig. 5, *c*. Generally, we may conclude that the increased values of both parameters are to a considerable extent spatially overlapped which is especially explicitly displayed for the Mongol-Okhotsk folded system and the Bureya massif, where the highest seismicity is observed. This specific feature is most likely associated with the occurrence of a relatively large number of weak earthquakes occurred in this region, which causes both complication of the structure of the epicentral field (frequently displayed in increasing D_e), and an increase in the recurrence plot slope b . However, such a correlation is not absolute.

5. CHARACTERISTICS OF SELF-SIMILARITY OF THE FAULT NETWORK

The analysis of the fractal dimension. To perform the analysis, we have calculated the fractal dimension of all the faults derived from the database from relation (3) using the FrAnGeo program [Zakharov, 2011, 2012] and

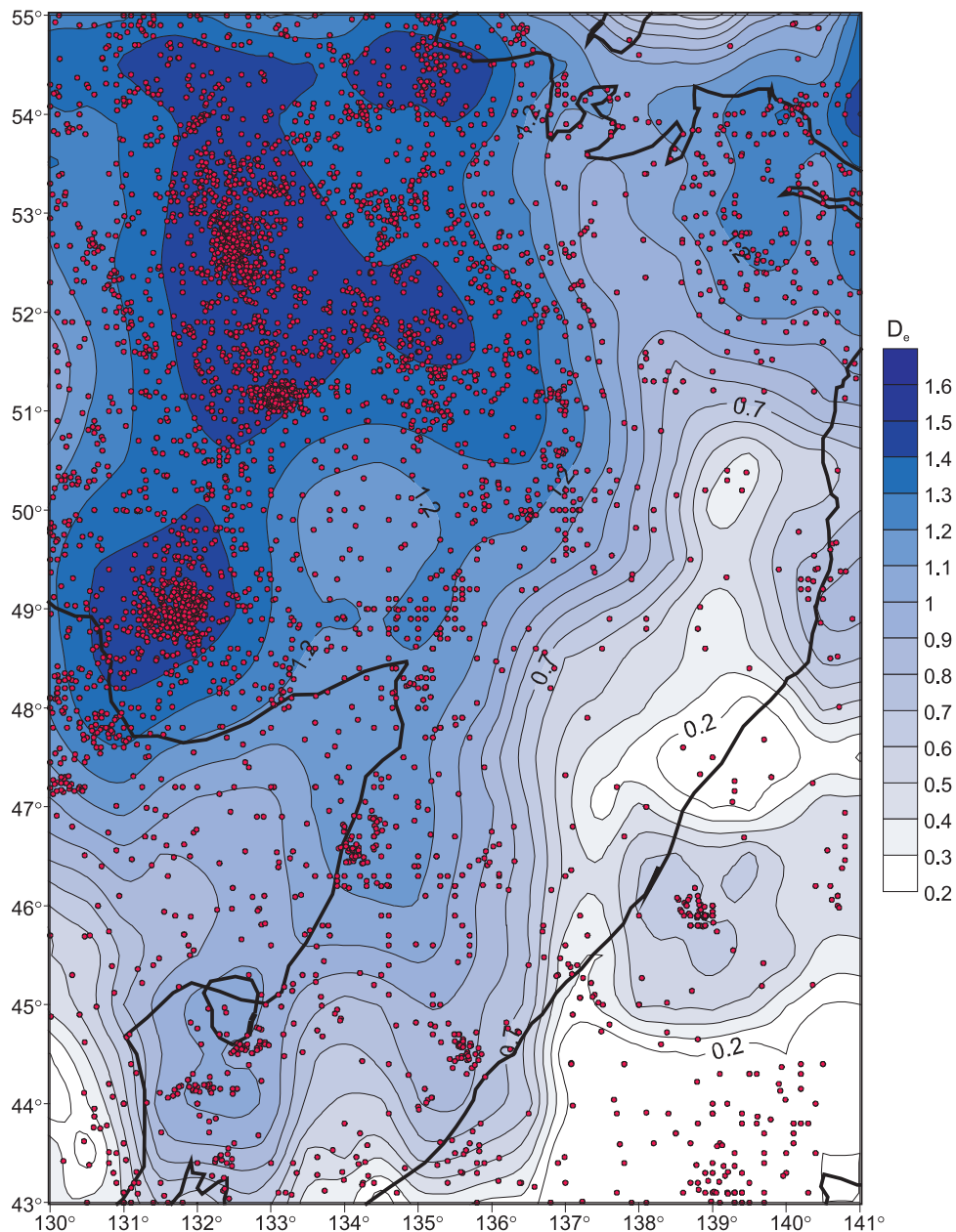


Fig. 4. Fractal dimension of the epicentral field of the upper crustal earthquakes D_e , calculated in the moving window.

Рис. 4. Фрактальная размерность поля эпицентров верхнекоровых землетрясений D_e , рассчитанная в скользящем окне.

the box-counting method. In the analysis, each fault was considered as a linear object not having its own structure. The range of box sizes used to calculate D_f varied from 4 to 0.0625° by latitude (approximately 315–5 km at a given latitude). According to our calculations, the fractal dimension of the fault network is $D_f=1.6\pm 0.03$ (see Fig. 2c; correlation coefficient $r=0.99$).

In order to reveal the spatial features of variations in the fractal dimension (Fig. 6), we performed more detailed moving window calculations using the author's FrAnGeo program as compared to our earlier calculations [Didenko *et al.*, 2017]). The window size

was 2° by latitude (160×160 km), a step was 0.5° (40 km) and the box sizes varied from 2 to 0.0625° by latitude (160–5 km).

We note that the fault data are irregular and are mainly available for the continental areas, the decreased values of the fractal dimension are observed in proximity to the continent-ocean boundary i.e., in the eastern part of the study area, as well as in its western part. This is, to a significant extent, due to the lack of data and a specific feature of the fractal analysis performed over a moving window and cannot be considered as evidence of a change of the fractal structure of faults in these zones.

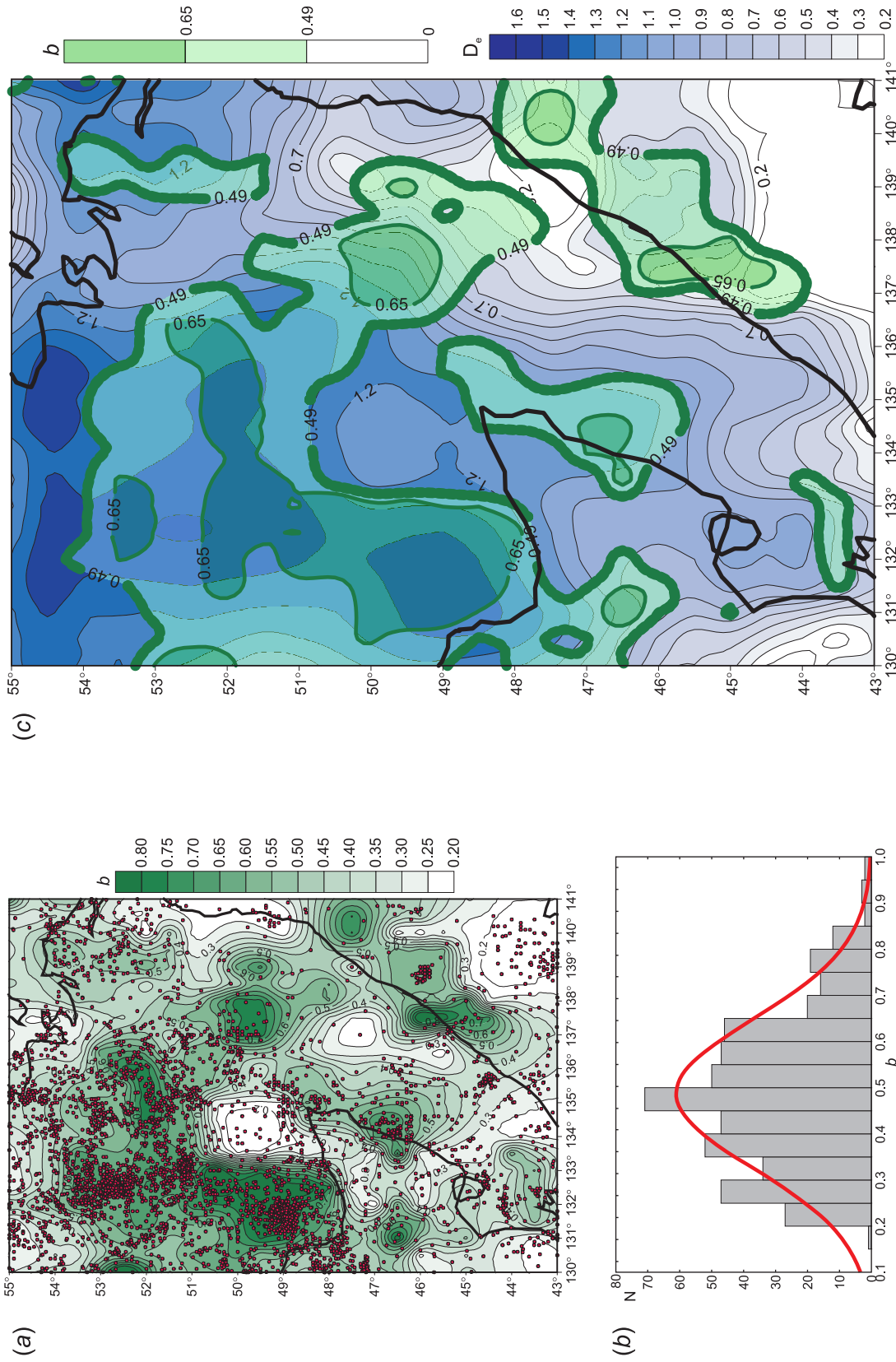


Fig. 5. The earthquake recurrence plot slope calculated in the moving window. (a) – *b*-value field for the upper crustal earthquakes; (b) – *b*-value statistics; (c) – the *b*-value spatial distribution vs. the distribution of the fractal dimension of earthquake epicenters D_e . Thick green line – average value $b=0.49$.

Рис. 5. Наклон графика повторяемости, рассчитанный в скользящем окне. (a) – поле *b* для верхнекоровых землетрясений; (b) – статистика значений *b*; (c) – сопоставление пространственного распределения *b* с распределением фрактальной размерности эпицентров D_e . Жирная зеленая линия – среднее значение $b=0.49$.

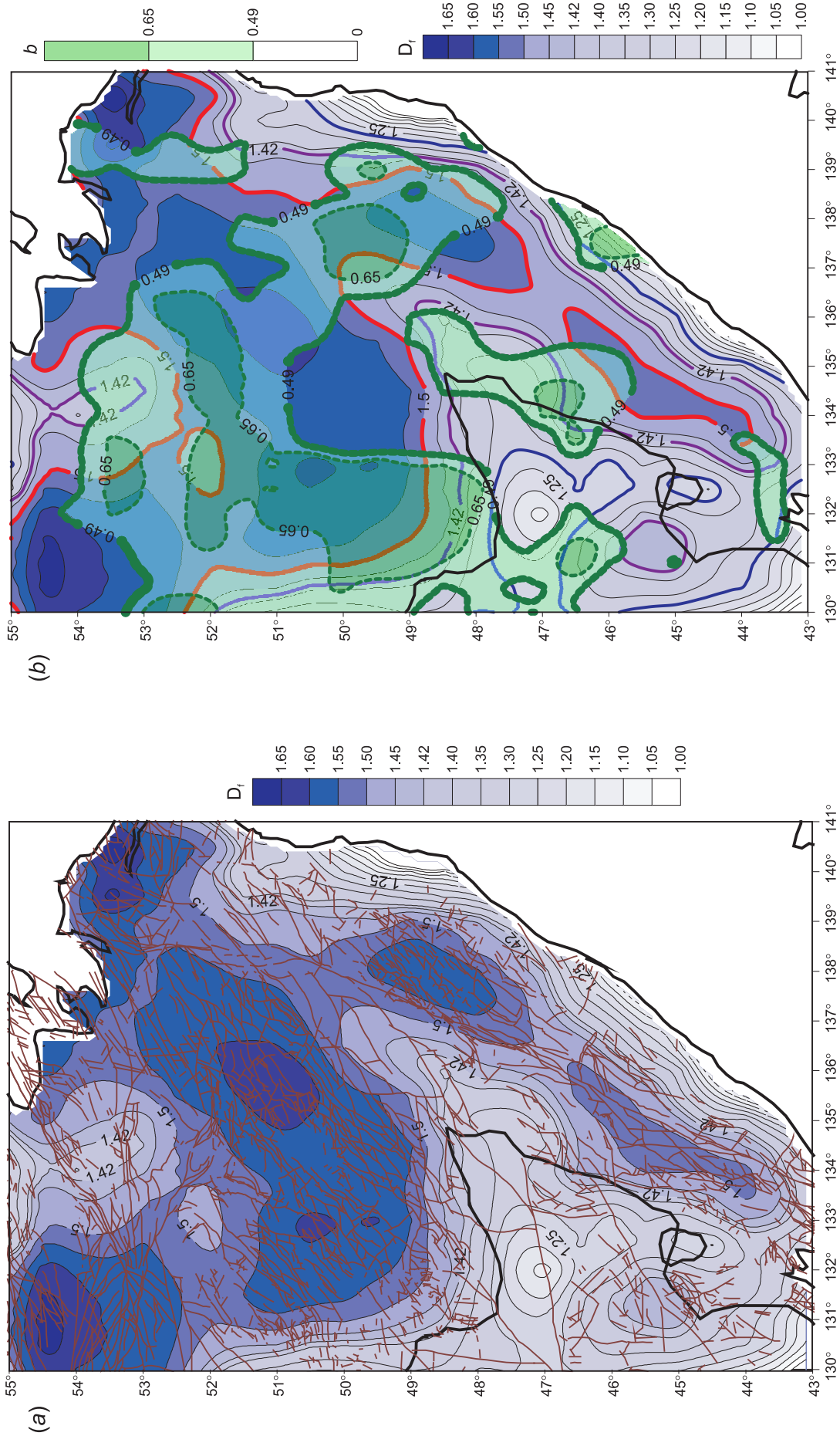


Fig. 6. Fractal dimension of the regional fault network D_f . (a) – D_f field calculated in the moving window. Brown lines – faults; (b) – comparison of the b spatial distribution for the upper crustal seismicity with D_f . Green line – $b=0.49$; red line – $D_f=1.5$.

Рис. 6. Фрактальная размерность (D_f) разломной сети региона b . (a) – поле D_f , рассчитанное в скользящем окне. Коричневые линии – разломы; (b) – сопоставление пространственного распределения параметра b для верхнекортовой сейсмичности с D_f . Зеленая линия – значение $b=0.49$, красная линия – значение $D_f=1.5$.

The distribution of D_f by value is complicated and differs strongly from the 'normal' one: the minimum value is 1.0, the maximum value is 1.69, the average value amounts to 1.41 ± 0.01 , the standard deviation is 0.15, the median of the distribution is 1.45, and the mode is 1.57. Simplification and generalization allowed for distinguishing three main ranges in the distribution of the fractal dimension values D_f , which are separated by considerable jumps in the frequency values and form the following steps in the distribution pattern: 1–1.3, 1.3–1.5 and 1.5–1.69. The first range ($D_f \leq 1.3$) is mainly linked to the above mentioned bands of low D_f values observed at the edges of the study area and cannot be comparable with the features of its structure based on these data. Therefore, we distinguish two main ranges of D_f values, considering a threshold value of 1.5. Note that this value differs considerably from the average value and is close to the median of the distribution, which is due to the observed asymmetry and causes the difference from the normal distribution of D_f values. In our opinion, the two distinguished ranges of D_f values correspond to different elements of the regional tectonic structure. Most probably, a discrepancy between the fractal dimension values for the faults of the Priamurye area (in our study, the maximum value is 1.65) and the previous results reported by *Sherman et al.* [2001] (1.55) is due to the difference in the input data, and, also, can be explained by somewhat different analysis techniques.

6. COMPARISON OF THE FRACTAL DIMENSION OF THE FAULT NETWORK WITH THE RECURRENCE PLOT SLOPE

The self-similar (fractal) properties of the seismic process and the medium, in which this process occurs, are expressed in parameters of the power laws that describe these properties: the fractal dimension values of the fault networks D_f , the epicentral (generally speaking, and the hypocentral) fields and parameter b in the Gutenberg-Richter law. For this reason, there are strong grounds to suggest a certain relationship between them. The supposed theoretical relationship between these values was described by *Kasahara* [1981] and *Turcotte* [1997]:

$$D_f = 3b/c, \quad (4)$$

where c is the parameter that relates the seismic moment and the magnitude (moment magnitude), b is the slope of the earthquake recurrence plot based on the moment magnitude M_w distribution. Assuming an average world value $c = 1.5$ [*Kasahara*, 1981], relation (4) is as follows:

$$D_f = 2b. \quad (5)$$

In the previous work by *Zakharov* [2011], the relations between b - and D_f were obtained from the seismotectonic analysis of Eurasia, which show that relation (5) approximately holds, but rather significant deviations are observed: for most regions and, on average, the coefficient relating D_f and b is somewhat higher than 2 and varies within the range of $1.7 \div 2.4$. Such a consistency between the fractal distribution of the earthquake magnitude (and, consequently, energy) and the fractal distribution of the fault sizes quantitatively confirms the hierarchical self-similar properties of the seismotectonic process.

Quite a great number of works have been published [e.g., *Oncel et al.*, 2001; *Caneva, Smirnov*, 2004; *Chen et al.*, 2006; *Stakhovsky*, 2004, 2017; and others], which describe practical studies and show a comparison between the fractal characteristics of the fault systems and seismicity in different regions of the world. These works demonstrate that relation (5) holds for the regions for quite a long time span, on average. At the same time, rather significant space-time variations, as well as variations due to features of the seismic regime, are possible in the relations between D_f and b . The performed experiments on the acoustic emission, which serves as a model of the seismic process, have yielded the relations between D_f and b close to 2 [*Goebel et al.*, 2017].

During the analysis, we compared the fractal dimension of the faults and the parameter b -values. Since we analyzed the surface fault system, it was reasonable to examine only the upper crustal seismicity.

The superposition of the above mentioned b -value field on the D_f -value field is illustrated in Fig. 6, *b*. To make comparison more convenient, the b -value field is shown in sparse isolines. The comparison of the fields of these parameters allows for revealing a general correlation between increased b -values (higher than an average value of 0.49) and increased D_f values. Undoubtedly, this relation does not hold strictly, and the inconsistency between the D_f minimum and b maximum values observed in the southern part of the Middle Amur depression is of special significance. We suggest that such inconsistency is caused by a relatively increased seismic activity associated with the Kharpi-Kur-Priamirye zone, but the faults are weakly displayed at the surface in this zone (as earlier discussed).

In our study, we investigated the correspondence of the calculated D_f and b -values to relation (5). It is necessary to take into consideration that this relation should (theoretically) hold for the recurrence plot slope based on the moment magnitude distribution of earthquakes (M_w), whereas the analyzed catalog lists the magnitudes obtained from surface waves (M_{LH}). Obviously, this distinction should influence the result: the coefficient of relation between D_f and b will be different from 2. To more adequately estimate relation

(5), we need to recalculate the magnitudes according to the scale and to calculate parameter b . To do this, we use the empirical relation between M_L and M_w , obtained by *Munafò et al. [2016]* based on the statistical analysis:

$$M_w = \begin{cases} 2/3M_L + C, & M_L \leq 4 \\ M_L, & M_L > 4 \end{cases} \quad (6)$$

where $C \approx 1.15$. Since according to [*Kononov, Sychev, 2014*]:

$$M_L = (0.97 \pm 0.04) \cdot M_{LH} + (0.04 \pm 0.16),$$

i.e., $M_{LH} \approx M_L$, we can use (6) to estimate M_w based on the M_{LH} data.

Given the magnitude recalculation according to (6), the statistical relation D_f/b tends to a 'theoretical' value of about 2, which is consistent with the previous results [*Zakharov, 2011*]. This relation is also close to 2, on average, but is somewhat higher.

Thus, we may conclude that the self-similar magnitude (and, as a consequence, energy) distribution of earthquakes is generally consistent with the fractal distribution of the fault sizes. This quantitatively confirms the hierarchical self-similar properties of the seismo-tectonic process.

7. COMPARISON OF SPATIAL VARIATIONS IN THE FRACTAL DIMENSION WITH THE MAIN TECTONIC STRUCTURES

The comparison of spatial distribution of the fractal dimension values for the fault network with the main tectonic structures of the region indicates a rather clear zonality and the confineness of certain ranges of D_f values to different structures. To simplify the scheme reading (Fig. 7), we distinguished only the main threshold isoline values.

The comparison with the structural scheme of the region [*Zabrodin et al., 2015; Zabrodin, 2017*] (see Fig. 7, *a*) and the neotectonic map [*Grachev, 1997*] shows that the increased D_f values are confined to the Phanerozoic folded systems: the Sikhote Alin (especially its central part) in the Central Sikhote Alin Fault zone, and the Mongol-Okhotsk in the South Tukuringra Fault zone and the Yitong-Yilan-Paukan fault convergence zone. The D_f values observed within these fold systems exceed the average value of $D_f=1.42$, and the value higher than 1.5 is typical of the greater part of these areas. The increased D_f values are also typical of the northern Bureya massif, and, to some extent, for the adjacent areas of the Jiamusi massif. The area exhibiting the highest values ($D_f=1.67-1.69$) is located in the northwest of the region, in areas of the Limurchan Fault, the Chayatyng and Chertov Ranges, and, also,

in the northwestern Dzhagdy Range. The decreased (lower than average) D_f values correlate quite well with the depression and trough areas. In the first place, it is the Middle Amur depression showing the lowest values ($D_f=1.2$). A relative local minimum is identified in areas of the Uda and Torom marginal troughs, although shifted with respect to the troughs which is probably related to their relatively small (on a scale of our analysis) sizes. In the eastern Sikhote Alin, the volcano-plutonic system also exhibits low values, but it is difficult to differentiate whether these values are due to the structural features of the fault system or, as mentioned above, can be explained by the lack of the input data.

The performed comparison helps us conclude that the increased values of the fractal dimension of the fault network are confined to the folded systems, while the decreased values correlate with the depressions and troughs. This is explained by the more intense fault formation in the folded systems due to active orogenic processes. In addition, the depressions have a thicker sedimentary cover, which prevents from distinguishing the fault structure of the basement. A certain shift of the D_f -field maxima and minima with respect to the structures, which are, in particular, of a small size, can probably be explained by specific features of the analysis technique – “smearing” of the values during the averaging over a moving window.

8. COMPARISON WITH THE CONTEMPORARY STRESS-STRAIN STATE OF THE CRUST

In this study, we also compared the results of the fractal analysis of the fault network with the data on the recent stress-strain state of the crust derived from different methods, mainly from the analysis and interpretation of the data obtained by different types of remote sensing of the Earth reported by other researchers. The relations between the stress fields and deformations restored using seismic and satellite data were considered in different publications [e.g., *Lukhnev et al., 2010; Petrov et al., 2008*].

Let us make comparison with the deformations revealed from the GPS data interpretation and analysis described in *Ashurkov et al. [2016]*, where the technique used is based on spline-interpolation with 30×30 km box, which corresponds to the scale and degree of detail of our analysis and makes it possible to compare the results. The comparison illustrates that in general, the areas exhibiting increased values of the fractal dimension of the fault network ($D_f \geq 1.5$) correlate with the areas of relatively increased strain rates and of the second invariant (intensity) of the strain rate tensor. This results from active different-scale faulting occurred directly in the areas of intense deformations, which is displayed in the number of faults and the increased values of D_f .

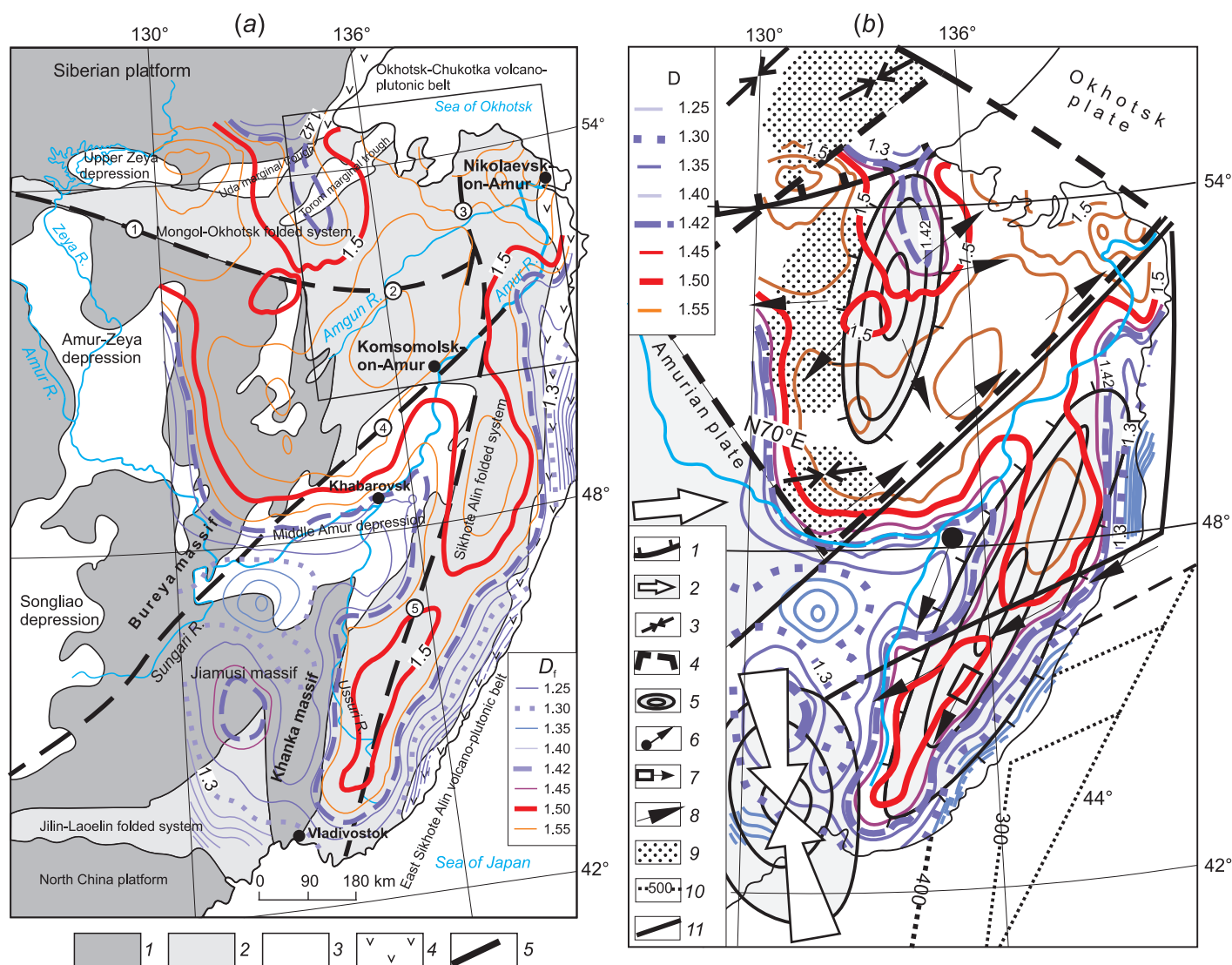


Fig. 7. Comparison of the calculated field of the fractal dimension of the fault network D_f with the geological and structural features of the region.

(a) – comparison with the structural scheme [Zabrodin, 2017]. Dashed blue line – $D_f=1.3$; hatched purple line – $D_f=1.42$; thick red line – $D_f=1.5$. For other explanations see Fig. 3.

(b) – comparison with the geodynamic and structural features of the buffer zone at the eastern front of the Amurian plate (modified after [Stepashko et al., 2018]). 1 – boundary of the Siberian platform; 2 – Amurian plate, the arrow shows its trajectory; 3 – directions of compression in the earthquake foci; 4 – boundaries of the Lower Amur crustal plate; 5 – main areas of compression (an abnormal seismicity zone at a depth of 500 km). The directions of the recent horizontal displacements according to GPS data: 6 – with respect to the Blagoveshchensk site, 7 – residual values of the displacement vectors; 8 – trajectories of earthquake migration along the boundary of the lithospheric block; 9 – clusters of weak earthquakes in Lower Priamurye; 10 – depth isolines of the subduction zone, km [Zhao, Tian, 2013]; 11 – boundaries of the lithospheric block.

Рис. 7. Сопоставление расчетного поля фрактальной размерности разломной сети (D_f) с геолого-структурными особенностями региона.

(а) – со структурной схемой региона [Zabrodin, 2017]. Пунктирная синяя линия соответствует значению $D_f=1.3$, штриховая фиолетовая – среднему значению $D_f=1.42$, соответствует жирная красная линия – значению $D_f=1.5$. Остальные условные обозначения см. на рис. 3.

(б) – сопоставление с геодинамикой и структурой буферной зоны на восточном фронте Амурской плиты, по [Stepashko et al., 2018] с изменениями. 1 – граница Сибирской платформы; 2 – Амурская плита, стрелка показывает ее траекторию; 3 – направления сжатия в очагах землетрясений; 4 – границы Нижнеамурской коровой пластины; 5 – главные области сжатия, зона аномальной сейсмичности на глубине 500 км. Направления современных горизонтальных перемещений по GPS данным: 6 – относительно пункта Благовещенска, 7 – остаточные значения векторов смещений; 8 – траектории миграции землетрясений вдоль границ литосферного блока; 9 – кластеры концентрации слабых землетрясений Нижнего Приамурья; 10 – изолинии глубины зоны субдукции, км [Zhao, Tian, 2013]; 11 – границы литосферного блока.

The comparison with the geodynamic analysis results obtained for the eastern edge of the Amurian plate by *Stepashko et al.* [2018], based on absolutely different methods – the analysis of seismotectonics and the recent crustal movements in the region, also indicates good consistency between the areas of increased fractal dimension values for the fault network ($D_f \geq 1.5$) and the main zones of compression (Fig. 7, *b*). This means that the fractal dimension of the fault network is one more important quantitative characteristic of fault intensity and the recent stress-strain state of the crust and can be used for the geodynamic analysis.

9. RESULTS AND CONCLUSIONS

We performed a comprehensive analysis of the characteristics of self-similarity of seismicity and the fault network within the Sikhote Alin orogenic belt and the adjacent areas. From the analysis results, and the comparison of the fields of the obtained characteristics of self-similarity between each other and with the structural, tectonic and geodynamic features of the region, the following conclusions can be made:

1) The depth distribution of earthquake foci and the geodynamic features of the region give grounds to claim that the main features of seismicity are controlled by the crustal and upper crustal earthquakes except for the area of deep-focal earthquakes related to the subduction zone in the Sea of Japan;

2) The fractal dimension of the field of earthquake epicenters of the region was calculated. Differentiation of the study area by the density of earthquake epicenters and the fractal dimension value D_e provides evidence that the most active crustal areas are linked to NE-trending Kharpi-Kur-Priamurye zone, that is the northern segment of the transregional Tan-Lu Fault System, the northern part of the Bureya massif, and the Mongol-Okhotsk folded system, which agrees with our previous results [*Didenko et al.*, 2017];

3) The earthquake recurrence plot slope b was estimated for the region. In general, its highest value correlates with the areas of the highest seismicity in the northern area of the Bureya massif and, to a lower extent, of the Mongol-Okhotsk folded system;

4) The field of the fractal dimension of the fault network D_f was calculated for the region. It has been

ascertained that the increased values of the fractal dimension of the fault network D_f are confined to the folded systems (Sikhote Alin and Mongol-Okhotsk), while the decreased D_f values correlate with the depressions and troughs (the Middle Amur depression, and, to a lower extent, the Uda and Torom marginal troughs). This is explained by a more intense faulting in the folded systems due to active orogenic processes;

5) The comparison of the fractal analysis results for the fault network with the data on the recent stress-strain state of the crust derived from different methods [*Rasskazov et al.*, 2014; *Ashurkov et al.*, 2016; *Stepashko et al.*, 2018] shows that the zones exhibiting the increased values of the fractal dimension of the fault network D_f are generally confined to the areas of contemporary compression. This makes the fractal analysis of the faults an important characteristic of the stress-strain state;

6) Good agreement has been revealed between the parameter b -value field for the upper crustal earthquakes and the field of the fractal dimension of the fault network D_f . We conclude that the self-similar distribution of earthquake magnitude (and, consequently, energy) is generally consistent with the fractal distribution of the fault sizes.

Our results show that the self-similarity parameters provide an important quantitative characteristic of fault intensity and the recent stress-strain state of the crust and can be used for the neotectonic and geodynamic analyses.

10. ACKNOWLEDGMENTS

The authors are thankful to reviewers Dr. A.V. Klyuchevskiy and Dr. V.B. Smirnov, whose constructive remarks and suggestions contributed to improving the quality of the final version of the manuscript, and E.Yu. Didenko and N.N. Kovriga, the staff members of the Institute of Tectonics and Geophysics, Far East Branch, Russian Academy of Sciences (ITiG FEB RAS), for their assistance in the preparation of the manuscript. The study was supported by the grant of the Russian Science Foundation (project No. 16-17-00015). The analysis was performed using high-performance computing systems of the Moscow State University Supercomputing Center [*Sadovnichy et al.*, 2013].

11. ЛИТЕРАТУРА / REFERENCES

- Ashurkov S.V., San'kov V.A., Serov M.A., Luk'yanov P.Yu., Grib N.N., Bordonskii G.S., Dembelov M.G.*, 2016. Evaluation of present-day deformations in the Amurian Plate and its surroundings, based on GPS data. *Russian Geology and Geophysics* 57 (11), 1626–1634. <https://doi.org/10.1016/j.rgg.2016.10.008>.
- Ben-Zion Y.*, 2008. Collective behavior of earthquakes and faults: Continuum-discrete transitions, progressive evolutionary changes, and different dynamic regimes. *Reviews of Geophysics* 46 (4), RG4006. <https://doi.org/10.1029/2008RG000260>.

- Caneva A., Smirnov V., 2004. Using the fractal dimension of earthquake distributions and the slope of the recurrence curve to forecast earthquakes in Colombia. *Earth Sciences Research Journal* 8 (1), 3–9.
- Chen C.-C., Wang W.-C., Chang Y.-F., Wu Y.-M., Lee Y.-H., 2006. A correlation between the b-value and the fractal dimension from the aftershock sequence of the 1999 Chi-Chi, Taiwan, earthquake. *Geophysical Journal International* 167 (3), 1215–1219. <https://doi.org/10.1111/j.1365-246X.2006.03230.x>.
- CRUST 2.0. A New Global Crustal Model at 2x2 Degrees. Available from: <http://igppweb.ucsd.edu/~gabi/crust2.html>.
- Didenko A.N., Kaplun V.B., Malyshev Yu.F., Shevchenko B.F., 2010. Lithospheric structure and Mesozoic geodynamics of the eastern Central Asian Fold Belt. *Russian Geology and Geophysics* 51 (5), 492–506. <https://doi.org/10.1016/j.rgg.2010.04.006>.
- Didenko A.N., Zakharov V.S., Gil'manova G.Z., Merkulova T.V., Arkhipov M.V., 2017. Formalized analysis of crustal seismicity in the Sikhote Alin Orogen and adjacent areas. *Russian Journal of Pacific Geology* 11 (2), 123–133. <https://doi.org/10.1134/S1819714017020026>.
- Earthquakes in Russia, 2006–2013. Available from: <http://www.gstras.ru/new/public/> (in Russian).
- Earthquakes in the USSR, 1962–1991. Available from: http://www.wdcb.ru/sep/seismology/cat_USSR.ru.html (in Russian).
- Earthquakes of North Eurasia, 1992–2013. Available from: <http://www.gstras.ru/new/public/> (in Russian).
- Goebel T.H.W., Kwiatek G., Becker T.W., Brodsky E.E., Dresen G., 2017. What allows seismic events to grow big? Insights from b-value and fault roughness analysis in laboratory stick-slip experiments. *Geology* 45 (9), 815–818. <https://doi.org/10.1130/G39147.1>.
- Gorelov P.V., Shkabarnya N.G., Nagornova N.A., 2016. Analysis of seismic activity and faults in Primorye. *International Research Journal* 7 (49), Part 4, 146–149 (in Russian) [Горелов П.В., Шкабарня Н.Г., Нагорнова Н.А. Анализ сейсмической активности и разрывных нарушений Приморского края // Международный научно-исследовательский журнал. 2016. № 7 (49). Часть 4. С. 146–149]. <https://doi.org/10.18454/IRJ.2016.49.068>.
- Goryainov P.M., Ivanyuk G.Yu., 2001. Self-Organization of Mineral Systems. GEOS, Moscow, 312 p. (in Russian) [Горяинов П.М., Иванюк Г.Ю. Самоорганизация минеральных систем. М.: ГЕОС, 2001. 312 с.].
- Grachev A.F. (Ed.), 1997. The Map of Recent Tectonics of Northern Eurasia. Scale of 1:5000000. Ministry of Natural Resources of the Russian Federation (MPR RF), Russian Academy of Sciences (in Russian) [Карта новейшей тектоники Северной Евразии. Масштаб: 1:5000000 / Ред. А.Ф. Грачев. МПР РФ, Российская Академия наук, 1997].
- Kasahara K., 1981. Earthquake Mechanics. Cambridge University Press, Cambridge, 272 p.
- Khanchuk A.I. (Ed.), 2006. Geodynamics, Magmatism and Metallogeny of Eastern Russia. Dalnauka, Vladivostok, 981 p. (in Russian) [Геодинамика, магматизм и металлогения востока России / Ред. А.И. Ханчук. Владивосток: Дальнаука, 2006. 981 с.].
- Klyuchevskiy A.V., Zuev F.L., Klyuchevskaya A.A., 2017. Patent for invention No. 2625627. Technique for determining the self-similarity indicator of the field of earthquake epicenters (in Russian) [Ключевский А.В., Зуев Ф.Л., Ключевская А.А. Патент на изобретение № 2625627. Способ определения показателя самоподобия поля эпицентров землетрясений. 2017].
- Kondorskaya N.V., Shebalin N.V. (Eds.), 1977. New Catalog of Strong Earthquakes for the USSR Territory from the Ancient Times up to 1975. Nauka, Moscow, 536 p. (in Russian) [Новый каталог сильных землетрясений на территории СССР с древнейших времен до 1975 г. / Ред. Н.В. Кондорская, Н.В. Шебалин. М.: Наука, 1977. 536 с.].
- Konovalov A.V., Sychev A.S., 2014. A calibration curve of local magnitude and intermagnitude relations for Northern Sakhalin. *Journal of Volcanology and Seismology* 8 (6), 390–400. <https://doi.org/10.1134/S0742046314060050>.
- Kossobokov V.G., Nekrasova A.K., 2004. The unified scaling law for earthquakes: the global map of parameters. In: V.I. Keilis-Borok, G.M. Molchan (Eds.), The analysis of geodynamic and seismic processes. *Vychislitel'naya seismologiya (Computational Seismology)*, vol. 35. GEOS, Moscow, p. 160–175 (in Russian) [Кособоков В.Г., Некрасова А.К. Общий закон подобия для землетрясений: глобальная карта параметров // Анализ геодинамических и сейсмических процессов / Ред. В.И. Кейлис-Борок, Г.М. Молчан. Вычислительная сейсмология. Вып. 35. М.: ГЕОС, 2004. С. 160–175].
- Levin B.V., Kim Chun Un, Nagornykh T.V., 2008. Seismicity of Primorye and Priamurye regions in 1888–2008. *Bulletin of the Far Eastern Branch of the Russian Academy of Sciences* (6), 16–22 (in Russian) [Левин Б.В., Ким Чун Ун, Нагорных Т.В. Сейсмичность Приморья и Приамурья в 1888–2008 гг. // Вестник ДВО РАН. 2008. № 6. С. 16–22].
- Lukhnev A.V., San'kov V.A., Miroshnichenko A.I., Ashurkov S.V., Calais E., 2010. GPS rotation and strain rates in the Baikal-Mongolia region. *Russian Geology and Geophysics* 51 (7), 785–793. <https://doi.org/10.1016/j.rgg.2010.06.006>.
- Mandelbrot B.B., 1983. The Fractal Geometry of Nature. W.H. Freeman and Company, New York, 468 p.
- Munafò I., Malagnini L., Chiaraluce L., 2016. On the relationship between M_w and M_L for small earthquakes. *Bulletin of the Seismological Society of America* 106 (5), 2402–2408. <https://doi.org/10.1785/0120160130>.

- Nava F.A., Márquez-Ramírez V.H., Zúñiga F.R., Ávila-Barrientos L., Quinteros C.B., 2017. Gutenberg-Richter b-value maximum likelihood estimation and sample size. *Journal of Seismology* 21 (1), 127–135. <https://doi.org/10.1007/s10950-016-9589-1>.
- Nekrasova A.K., Kossobokov V.G., 2005. Temporal variations in the parameters of the unified scaling law for earthquakes in the eastern part of Honshu Island (Japan). *Doklady Earth Sciences* 405 (9), 1352–1356.
- Nekrasova A.K., Kossobokov V.G., Parvez I.A., 2015. Seismic hazard and seismic risk assessment based on the unified scaling law for earthquakes: Himalayas and adjacent regions. *Izvestiya, Physics of the Solid Earth* 51 (2), 268–277. <https://doi.org/10.1134/S1069351315010103>.
- Nikolaev V.V., 1992. Tan-Lu–Kur fault: basement structure and seismicity. In: Problems of tectonics, and energy and mineral resources. Amurian Division of the USSR Geographical Society, Far East Branch of RAS, Khabarovsk, p. 81–92 (in Russian) [Николаев В.В. Танлу-Курский разлом: структура фундамента и сейсмичность // Проблемы тектоники, энергетические и минеральные ресурсы. Хабаровск: Приамурский филиал Географического общества СССР, ДВО РАН, 1992. С. 81–92].
- Öncel A.O., Wilson T.H., Nishizawa O., 2001. Size scaling relationships in the active fault networks of Japan and their correlation with Gutenberg-Richter b values. *Journal of Geophysical Research: Solid Earth* 106 (B10), 21827–21841. <https://doi.org/10.1029/2000JB900408>.
- Ovsyuchenko A.N., Trofimenko S.V., Novikov S.S., Didenko A.N., Imaev V.S., 2018. The problems of seismic risk prediction for the territory of the Lower Amur Region: paleoseismological and seismological analysis. *Russian Journal of Pacific Geology* 12 (2), 135–150. <https://doi.org/10.1134/S1819714018020045>.
- Petrov V.A., Anfu N., Smirnov V.B., Mostryukov A.O., Zhixiong L., Ponomarev A.V., Zaisen J., Xuhui S., 2008. Field of tectonic stresses from focal mechanisms of earthquakes and recent crustal movements from GPS measurements in China. *Izvestiya, Physics of the Solid Earth* 44 (10), 846–855. <https://doi.org/10.1134/S1069351308100121>.
- Rasskazov I.Yu., Saksin B.G., Petrov V.A., Shevchenko B.F., Usikov V.I., Gil'manova G.Z., 2014. Present-day stress-strain state in the upper crust of the Amurian lithosphere plate. *Izvestiya, Physics of the Solid Earth* 50 (3), 444–452. <https://doi.org/10.1134/S1069351314030082>.
- Rautian T.G., Khalturin V.I., Fugita K., Mackey K.G., Kendall A.D., 2007. Origins and methodology of the Russian energy K-class system and its relationship to magnitude scales. *Seismological Research Letters* 78 (6), 579–590. <https://doi.org/10.1785/gssrl.78.6.579>.
- Robertson M.C., Sammis C.G., Sahimi M., Martin A.J., 1995. Fractal analysis of three-dimensional spatial distributions of earthquakes with a percolation interpretation. *Journal of Geophysical Research: Solid Earth* 100 (B1), 609–620. <https://doi.org/10.1029/94JB02463>.
- Sadovnichy V., Tikhonravov A., Voevodin V., Opanasenko V., 2013. “Lomonosov”: supercomputing at Moscow State University. In: Contemporary High Performance Computing. Chapman and Hall/CRC, Boca Raton, USA, p. 283–307.
- Sadovsky M.A., 2004. Selected Contributions: Geophysics and Physics of Explosion. Nauka, Moscow, 439 p. (in Russian) [Садовский М.А. Избранные труды: Геофизика и физика взрыва. М.: Наука, 2004. 439 с.].
- Sadovsky M.A., Pisarenko V.F., 1991. Seismic Process in the Block Medium. Nauka, Moscow, 96 p. (in Russian) [Садовский М.А., Писаренко В.Ф. Сейсмический процесс в блоковой среде. М.: Наука, 1991. 96 с.].
- Safonov D.A. 2018. Seismic activity of the Amur and Primorye. *Geosystems of Transition Zones* 2 (2), 104–115 (in Russian) [Сафонов Д.А. Сейсмическая активность Приамурья и Приморья // Геосистемы переходных зон. 2018. Т. 2. № 2. С. 104–115]. <https://doi.org/10.30730/2541-8912.2018.2.2.104-115>.
- Sherman S.I., 2005. The nonstationary tectonophysical model of faults and its application to analysis of the seismic process in destructive zones of the lithosphere. *Fizicheskaya Mezomechanika (Physical Mesomechanics)* 8 (1), 71–80 (in Russian) [Шерман С.И. Нестационарная тектонофизическая модель разломов и ее применение для анализа сейсмического процесса в деструктивных зонах литосферы // Физическая мезомеханика. 2005. Т. 8. № 1. С. 71–80].
- Sherman S.I., 2012. Destruction of the lithosphere: fault-block divisibility and its tectonophysical regularities. *Geodynamics & Tectonophysics* 3 (4), 315–344. (in Russian) [Шерман С.И. Деструкция литосферы: разломно-блоковая делимость и ее тектонофизические закономерности // Геодинамика и тектонофизика. 2012. Т. 3. № 4. С. 315–344]. <https://doi.org/10.5800/GT-2012-3-4-0077>.
- Sherman S.I., 2014. Seismic Process and the Forecast of Earthquakes: Tectonophysical Conception. Academic Publishing House GEO, Novosibirsk, 359 p. (in Russian) [Шерман С.И. Сейсмический процесс и прогноз землетрясений: тектонофизическая концепция. Новосибирск: Академическое изд-во «ГЕО», 2014. 359 с.].
- Sherman S.I., Sorokin A.P., Cheremnykh A.V., 2001. A new approach to tectonic regionalization of the Amur Region based on the fractal dimension of crustal faults. *Doklady Earth Sciences* 381A (9), 1020–1024.
- Stakhovskiy I.R., 2004. Interrelation between spatial and energy scalings of the seismic process. *Izvestiya, Physics of the Solid Earth* 40 (10), 849–855.
- Stakhovskiy I.R., 2017. Scale invariance of shallow seismicity and the prognostic signatures of earthquakes. *Physics-Uspokhi* 60 (5), 472–489. <https://doi.org/10.3367/UFNe.2016.09.037970>.
- Stepashko A.A., Merkulova T.V., Didenko A.N., 2018. Geodynamics and regularities of seismicity in the eastern segment of the Amurian Plate. *Russian Journal of Pacific Geology* 12 (4), 263–277. <https://doi.org/10.1134/S1819714018040061>.

- Torabi A., Berg S.S., 2011. Scaling of fault attributes: A review. *Marine and Petroleum Geology* 28 (8), 1444–1460. <https://doi.org/10.1016/j.marpetgeo.2011.04.003>.
- Turcotte D.L., 1997. *Fractals and Chaos in Geology and Geophysics*. 2nd edition. Cambridge University Press, Cambridge, 398 p.
- Ulomov V.I., 2009. Estimation of seismic hazard in the Primorye region. *Inzhenernye Izyskaniya* (1), 40–47 (in Russian) [Уломов В.И. К оценке сейсмической опасности территории Приморского края // *Инженерные изыскания*. 2009. № 1. С. 40–47].
- Zabrodin V.Yu., 2017. Tectonics and evolution of the northeastern extremity of the East-Asian Rift Belt. *Russian Journal of Pacific Geology* 11 (3), 155–162. <https://doi.org/10.1134/S1819714017030071>.
- Zabrodin V.Yu., Rybas O.V., Gil'manova G.Z., 2015. Fault Tectonics of the Russian Far East Mainland. Dalnauka, Vladivostok, 132 p. (in Russian) [Забродин В.Ю., Рыбас О.В., Гильманова Г.З. Разломная тектоника материковой части Дальнего Востока России. Владивосток: Дальнаука, 2015. 132 с.].
- Zakharov V.S., 2011. Analysis of the characteristics of self similarity of seismicity and the active fault network of Eurasia. *Moscow University Geology Bulletin* 66 (6), 385–392. <https://doi.org/10.3103/S0145875211060123>.
- Zakharov V.S., 2012. Preliminary analysis of the self-similarity of the aftershocks of the Japanese earthquake on March 11, 2011. *Moscow University Geology Bulletin* 67 (2), 133–137. <https://doi.org/10.3103/S0145875212020081>.
- Zhao D., Tian Y., 2013. Changbai intraplate volcanism and deep earthquakes in East Asia: a possible link? *Geophysical Journal International* 195 (2), 706–724. <https://doi.org/10.1093/gji/ggt289>.

INFORMATION ABOUT AUTHORS | СВЕДЕНИЯ ОБ АВТОРАХ


Vladimir S. Zakharov

Doctor of Geology and Mineralogy, Professor

M.V. Lomonosov Moscow State University, Faculty of Geology
1 Leninskie Gory, GSP-1, Moscow 119991, Russia

Dubna State University
19 Universitetskaya street, Dubna 141982, Russia

✉ e-mail: zakharov@geol.msu.ru

 <https://orcid.org/0000-0002-8888-4239>

Владимир Сергеевич Захаров

докт. геол.-мин. наук, профессор

Московский государственный университет им. М.В. Ломоносова,
геологический факультет
119991, Москва, Ленинские Горы, 1, Россия

Государственный университет «Дубна»
141982, Дубна, ул. Университетская, 19, Россия


Aleksei N. Didenko

Doctor of Geology and Mineralogy, Corresponding Member of RAS,
Chief Researcher

Yu.A. Kosygin Institute of Tectonics and Geophysics, Far East Branch of RAS
65 Kim Yu Chen street, Khabarovsk 680000, Russia

Pacific National University
136 Tikhookeanskaya street, Khabarovsk 680035, Russia

e-mail: itig@itig.as.khb.ru

 <https://orcid.org/0000-0003-4249-3985>

Алексей Николаевич Диденко

докт. геол.-мин. наук, член-корреспондент РАН, г.н.с.

Институт тектоники и геофизики им. Ю.А. Косыгина ДВО РАН
680000, Хабаровск, ул. Ким Ю Чена, 65, Россия


Тихоокеанский государственный университет
680035, Хабаровск, ул. Тихоокеанская, 136, Россия

Gul'shat Z. Gil'manova

Candidate of Geology and Mineralogy, Senior Researcher,
Head of GIS Department

Yu.A. Kosygin Institute of Tectonics and Geophysics, Far East Branch of RAS
65 Kim Yu Chen street, Khabarovsk 680000, Russia

e-mail: gigulya@yandex.ru

 <https://orcid.org/0000-0003-1382-9742>

Гульшат Забировна Гильманова

канд. геол.-мин. наук, с.н.с., зав. группы ГИС


Институт тектоники и геофизики им. Ю.А. Косыгина ДВО РАН
680000, Хабаровск, ул. Ким Ю Чена, 65, Россия

Tatiana V. Merkulova

Candidate of Geology and Mineralogy, Lead Researcher

Yu.A. Kosygin Institute of Tectonics and Geophysics, Far East Branch of RAS
65 Kim Yu Chen street, Khabarovsk 680000, Russia

e-mail: merkulova@itig.as.khb.ru

 <https://orcid.org/0000-0003-1283-5032>

Татьяна Владимировна Меркулова

канд. геол.-мин. наук, в.н.с.

Институт тектоники и геофизики им. Ю.А. Косыгина ДВО РАН
680000, Хабаровск, ул. Ким Ю Чена, 65, Россия